Journal of Membrane Science 427 (2013) 85–91

Contents lists available at SciVerse ScienceDirect

Journal of Membrane Science

journal homepage: www.elsevier.com/locate/memsci

Direct sulfonation and photocrosslinking of unsaturated poly(styrene-*b*-butadiene-*b*-styrene) for proton exchange membrane of direct methanol fuel cell

Seulgi Kim [a], Hyunjung Lee [b], Dahee Ahn [a], Hae Woong Park [c], Taihyun Chang [c], Wonmok Lee [a,*]

[a] Department of Chemistry, Sejong University, 98 Gunja-dong, Gwangjin-gu, Seoul 143-747, Republic of Korea
[b] School of Advanced Materials Engineering, Kookmin University, 861-1 Jeongneung-Dong, Seoul 136-702, Republic of Korea
[c] Department of Material Science and Engineering, Pohang University of Science and Technology, San 31 Hyoja-dong, Pohang 790-784, Republic of Korea

ARTICLE INFO

Article history:
Received 31 May 2012
Received in revised form
31 August 2012
Accepted 2 September 2012
Available online 2 October 2012

Keywords:
Proton exchange membrane
SBS
Sulfonation
Block copolymer
Crosslinking
Direct methanol fuel cell

ABSTRACT

In this report, we demonstrate a simple preparation of the partially sulfonated poly(styrene-*b*-butadiene-*b*-styrene) (sSBS), casting and photocrosslinking of tough films which can be used as a proton exchange membrane (PEM) for direct methanol fuel cell (DMFC). Upon reaction with acetylsulfate in a homogeneous solution phase, SBS was converted to sSBS with a degree of sulfonation (DS) in a controlled manner. Subsequent washing and redissolution of the product in the mixed solvent enabled the solution casting of the mechanically stable membranes, which could be further toughened by crosslinking the butadiene groups with the premixed divinylbenzene (DVB) upon exposure to UV light. The sSBS membranes showed excellent proton conductivity as well as low methanol permeability presumably due to the efficient formation of hydrophilic channels aided by microphase separation. The nanostructures of the sSBS PEMs were rigorously characterized by the small angle X-ray scattering (SAXS) and electron microscopic analyses. Finally the membrane electrode assembly (MEA) was fabricated using the sSBS as PEM, and an active mode DMFC test was performed to show a power density of a single cell containing noncrosslinked sSBS to be ~80 mW/cm^2 at 60 °C which is 15% higher than that of Nafion115-containing single cell under the same test conditions.

1. Introduction

Due to multiple advantages such as small device volume, simple fuel storage and supply, and low operation temperature, extensive work has been devoted to the development of direct methanol fuel cell (DMFC) as an electrical energy source for small mobile devices [1]. Membrane electrode assembly (MEA) is a core part of DMFC, in which a proton exchange membrane (PEM) selectively conducts protons from anode to cathode. Protons are usually moving through the hydrophilic channels within the PEM in the form of hydronium (H_3O^+) ions, while methanol, the liquid fuel of the DMFC, can also be permeating together with water molecules and hydronium ions which will inevitably lower the theoretical electromotive force. Hence, high proton conductivity and low methanol crossover are the most important membrane properties for a PEM of DMFC to determine overall energy conversion efficiency of the fuel cell [2]. In addition to proton conductivity and resistivity to fuel crossover, durability and processing cost are also prerequisite characteristics for PEM. Nafion™, a perfluorinated membrane manufactured by Dupont, has been the most frequently used PEM for both PEMFC and DMFC due to its superior chemical/mechanical stability and high proton conductivity [3,4]. However, its high methanol permeability is the biggest hurdle for practical application in DMFC. There have been efforts to solve the fuel crossover problem of Nafion by incorporating inorganic nanocomposite materials as a methanol barrier, [5,6] but development of hydrocarbon membrane is generally accepted to be the fundamental solution. One approach is to utilize the sulfonated form of the non-perfluorinated, but chemically stable polymers such as polystyrene (PS), [7] poly(ether ether ketone) (PEEK), [8,9] polyimide, [10] poly(phenyleneoxide), [11] poly(ether sulfone) (PES) [12–15]. Another fascinating idea to reduce methanol crossover through PEM is to utilize the nanostructured morphology of the block copolymer (BCP) generated by thermodynamically induced microphase separation [2,16–20]. By cautiously controlling BCP microphase separation, Park et al. achieved the different ion conductivities along different direction (through-plane vs. in-plane) of BCP orientation [21,22]. Well-controlled formation of proton conducting channels in BCP have shown promising PEM

* Corresponding author. Tel.: +82 2 3408 3212; fax: +82 2 3408 4317.
E-mail address: wonmoklee@sejong.ac.kr (W. Lee).

0376-7388/$ - see front matter © 2012 Elsevier B.V. All rights reserved.
http://dx.doi.org/10.1016/j.memsci.2012.09.008

properties for DMFC. In BCP PEM, sulfonated PS serves as hydrophilic domains and hydrophobic rubbery blocks such as polyisobutylene (PI) [2,16], poly(ethylene-ran-butylene) [17], polybutadiene (PB) [23], or poly(dimethylsiloxane) (PDMS) [18,19] provide processibility for the membrane casting as well as efficient formation of proton channels. From the manufacturing standpoint, SBS is a good candidate for BCP PEM due to a relatively low price (~$1.50/lb) and a large production (>10Mtons/year) worldwide [24]. Until now, sulfonated SBS (sSBS) has been rarely utilized as PEM materials for fuel cell owing to undesirable gelation during sulfonation process or because of membrane degradation caused by photolysis or chemolysis of unreacted double bonds. Nevertheless, there are some successful reports such as that of the sulfonated membrane of hydrogenated SBS which was applied to PEM for PEMFC [25,26]. Won and coworkers reported the post-sulfonation of the crosslinked SBS membrane for DMFC application [23].

In this report, we investigate direct sulfonation of prestine SBS and membrane casting to test a feasibility of BCP PEM manufacturing process for DMFC. We also study photo-crosslinking of the double bonds in PB block in order to improve mechanical property of the cast membrane.

2. Experimental

2.1. Materials

SBS (M_w~140,000 g/mol; 29 wt% styrene; Aldrich) was purified by reprecipitation to remove unwanted additives. Supporting data Fig. S1-1 shows the 1H-NMR spectrum in $CDCl_3$ of a purified SBS, and S1-2 shows a phase image of SBS film cast from toluene solution using tapping mode atomic force microscopy (Digital instruments) from which cylindrical BCP morphology is evident. Nafion™ dispersion (10 di%, E.W. 1100) was purchased from Dupont. Irgacure-651 (Ciba Specialty Chemicals), as a photoinitiator, divinylbenzene (DVB, Aldrich) as a crosslinker, tetrahydrofuran (THF, Samchun, 99.0%), methanol (Duksan, 99.8%), dichloroethane (DCE, Dae jung, 99%), sulfuric acid (Aldrich, 95–98%), acetic anhydride (Samchun, 99.0%), 2-propanol (IPA, Duksan, 99.5%), toluene (Aldrich, 99.5%), *n*-butyl alcohol (Duksan, 99%) were purchased and used without further purification.

2.2. Sulfonation of SBS

Five grams of SBS powder and 120 mL of DCE were added in a 3-neck round-bottomed flask at 40 °C which had been purged with nitrogen gas for 1 h. The polymer solution was stirred for another hour. Meanwhile, 3.6 g of acetic anhydride was slowly added in the mixture of 1.7 g sulfuric acid and 18 g of DCE in an ice bath to form acetyl sulfate. A measured amount of acetyl sulfate was added to the polymer solution at 0 °C, and the mixture was vigorously stirred using mechanical stirrer for 3 h. Upon completion of the sulfonation reaction, 10 mL IPA was added, and most of the liquid was removed by rotary evaporation. Crude product was washed with water and methanol repeatedly for several days until the pH became no less than 4. The purified sSBS was dried in a vacuum oven at room temperature [27]. Five samples with different degree of sulfonation (DS) were obtained.

2.3. Membrane preparation

The weighed sSBS was added in a mixed solvent of toluene/2-butanol (7/3) at 2.5 wt%, and the polymer was thoroughly dissolved by stirring for 1 week. The remaining non-dissolved product was filtered out by using a 200 mesh, and the filtrate was poured to a glass petri dish and slowly dried at 40 °C in a casting chamber. A sSBS solution and a cast membrane are shown in Fig. S2. Upon solution casting, a tough membrane was obtained without pin-holes as shown in Fig. S3 where the scanning electron micrographs of both pristine SBS and sSBS membranes are shown. For fabrication of a crosslinked membrane, the measured amounts of Irgacure-651 and DVB were premixed with polymer solution, and the dried membrane was placed under a UV-lamp (SB-100P/F, Spectronics Corp.) operating at 365 nm wavelength for 2 h. The cast membrane was soaked in deionized (DI) water until it was delaminated from the dish.

2.4. Characterizations of sSBS PEM

Sulfonation of an sSBS PEM was characterized using Fourier Transform Infra-red (FTIR) spectrometer (spectrum100, Perkin Elmer) by taking transmission spectrum of a membrane. The DS of each sSBS product was determined using elemental analysis and glass transition temperature (T_g) of the product was measured by differential scanning calorimetry (DSC, N-650, Scinco) after completely drying in a vacuum oven at 60 °C. Thermal degradation of sSBS was measured using Thermogravimetric analysis (TGA) apparatus (1100SF, Mettler-Toledo). In order to investigate the microstructure of the membrane, small angle X-ray scattering (SAXS) measurement was performed on wet or dried membrane using 4C1 SAXS beam-line at Pohang synchrotron light source. A wet PEM sample was prepared by soaking it in DI water at room temperature overnight. For a SAXS measurement, the membrane sample was cut and stacked to 0.2 mm thickness, and wrapped with Kapton™ tape leaving a small hole at the center for X-ray beam to pass through. The wavelength of the X-ray beam was 1.21 Å with an average energy of 0.26 keV. Proton conductivity of the PEM was determined by clipping $1\times4\ cm^2$ strip of a PEM to a home-made four-point prove conductivity cell and biasing AC current from an impedance analyzer (compactstat, IVIUM) in a temperature-stabilized water bath with a relative humidity of 100% [28]. The proton conductivity (σ) was calculated using a relationship $\sigma=L/(A\times R)$, where L and A are the distance between the two inner Pt-probes and the cross-sectional area of the membrane, respectively. Water uptake of a PEM was determined by immersing it into D.I. water for 24 h at room temperature, then rapidly wiping off the water on the membrane surface and weighing the swollen PEM until the weight of the PEM did not change. Finally, the wet PEM was dried in a vacuum oven at 70 °C for 24 h. The final dried weight of the PEM was measured and water uptake ($(W_{wet}-W_{dried})/W_{dried}$) was calculated. Dimensional changes of PEMs by drying were also measured, and the resulting water swelling data ($(L_{wet}-L_{dried})/L_{dried}$) are summarized in Table 1. Methanol permeability of a membrane was measured using a home-made diffusion cell, [29,30] and calculated according to the following equation.

$$DK=\frac{C_A}{C_B}\times\left(\frac{L\times V_B}{A}\right)\times\left(\frac{1}{t-t_0}\right)$$

where C_A and C_A are the concentration at two compartments, A and L are an area and a thickness of PEM, D and K are methanol diffusivity and distribution coefficient, and t is time. The DK value stands for the liquid's permeability through the membrane, i.e., the methanol crossover [20].

Tensile property of a membrane was measured using a universal testing machine (UTM, seris5567, Instron) [31]. $1\times4\ cm^2$ strip of a wet membrane was clipped on UTM and the strain–stress curve was measured. Oxidative stability was tested by soaking a small piece of membrane in Fenton's reagent (3% H_2O_2+2 ppm $FeSO_4$) at room temperature and monitoring the crack formation.

Table 1
Summary of membrane properties of crosslinked sSBS-58% ionomers used in this study.

Crosslinker content (%)	Proton conductivity (10^{-2} S/cm)	MeOH permeability (10^{-7} cm^2/s)	Water uptake (%)	Water swelling (%)	Tensile stress (N/mm^2)	Oxidative life-time (h)	Membrane selectivity[a]
(Nafion115)	9.0	27.0	26.7	9.5	13.9	N.A.	1
DVB-0%	4.5	8.6	75.1	20.3	4.6	8.5	1.6
DVB-2%	3.1	3.4	35.8	8.0	11.0	10.3	2.7
DVB-5%	3.4	6.6	23.9	7.98	13.9	12.3	1.5
DVB-10%	2.5	4.3	25.2	7.98	17.3	14.3	1.8

*All the measurements were carried out at room temperature except proton conductivity (30 °C).

[a] Normalized to the value of Nafion 115.

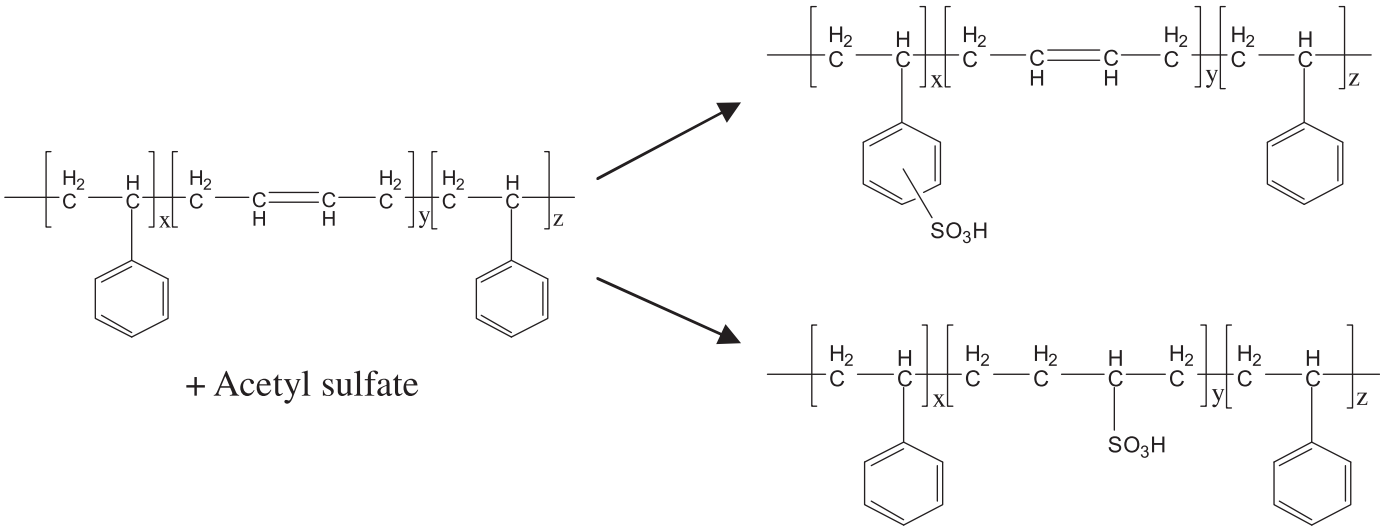

Scheme 1.

2.5. MEA fabrication and DMFC performance test

MEA was prepared by the following procedures. Catalyst slurries were prepared using Pt powder (Johnson-Matthy HIGH-SPEC 4000) for cathode and Pt/Ru powder (Johnson-Matthy HIGHSPEC 12100) for anode respectively. In preparation of both slurries, 20 wt% of Nafion ionomer was mixed as a binder. Catalyst loading for anode was 2 mg/cm^2 on Toray 060, and cathode loading was 2 mg/cm^2 on SGL-25BC. An MEA with a wet PEM with 3×3 cm^2 active area was hot-pressed at 80 °C for 1 min under 5 MPa pressure. For and Active mode DMFC performance test, 1 M methanol was supplied to anode by 3 mL/min flow rate, and air was supplied to cathode at the rate of 400 mL/min. After activation for several hours, the polarization curve was obtained at the temperature range of 30 °C to 60 °C.

3. Results and discussion

Acetyl sulfate is a well-known mild sulfonation agent for PS-containing BCPs. As for SBS, PB block is usually hydrogenated prior to sulfonation in order to prevent gelation of the sulfonated products [25,26]. In this study, however, the prestine SBS was directly sulfonated without hydrogenation which requires a catalytic reaction with pressurized hydrogen gas supply. Although the gel-like product was obtained upon sulfonation, subsequent evaporation of the volatile solvent and washing with water resulted in brown latex-like precipitates. The sulfonation reaction of SBS with acetyl sulfate may proceed in two different ways (Scheme 1). As shown in Fig. 1, FT-IR spectra of the reacted SBS showed symmetric and unsymmetric stretching peaks of sulfonic acid groups at 1150 cm^{-1} and 1040 cm^{-1}, respectively, which demonstrate a successful sulfonation of the polymer chain [26,32]. However, as shown in Scheme 1, acetyl sulfate can either sulfonate the phenyl group of PS or react with double bonds in the PB unit. As shown in Fig. 1, the characteristic absorption peaks of carbon–carbon double bonds from the PB unit were observed at 1600 cm^{-1} and 3000 cm^{-1} after sulfonation reaction reflecting that the majority of PB double bonds are still alive [33]. Once the

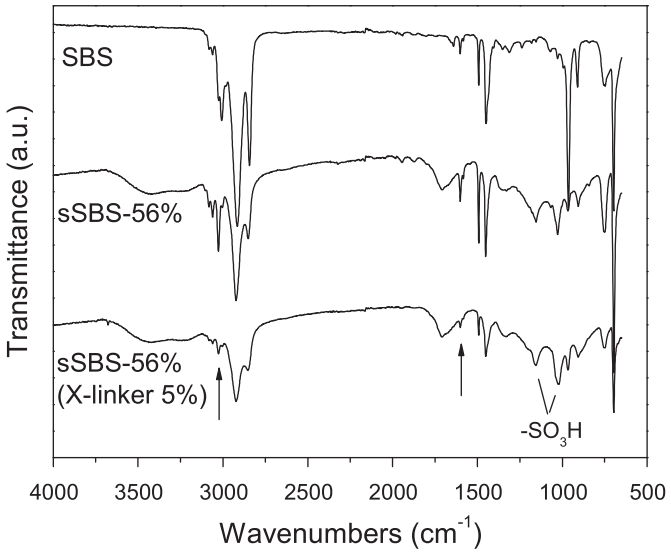

Fig. 1. FT-IR spectra of the membranes cast from SBS, sSBS-56% and a crosslinked sSBS-56%.

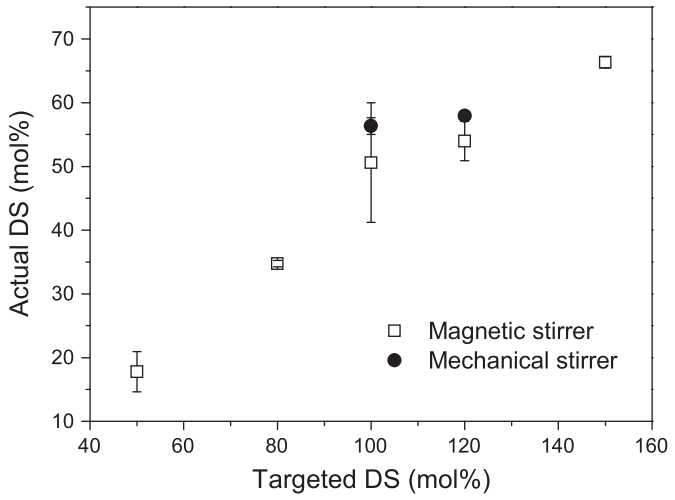

Fig. 2. Actual DS (mol%) of PS block vs. acetyl sulfate mol % in the reaction mixture. Actual DS was measured by elemental analysis.

sSBS was crosslinked by premixed DVB, the peak intensities of the unsaturated PB unit were significantly diminished as indicated by arrows in Fig. 1.

By varying acetyl sulfate content in the reaction mixture, DS of the PS blocks could be controlled. Elemental analyses on five different products apparently exhibited increases in actual DS as shown in Fig. 2. For instance, acetyl sulfate of 50 mol% with respect to PS content of SBS in the reaction mixture resulted in 18 mol% of the sulfonated PS block. By mixing 120 mol% of acetyl sulfate, ~52 mol% of DS was obtained. For convenience, sSBS-52% denotes the sSBS ionomer with actual DS of 52%. As shown in Fig. 2, the relationship of actual DS vs. target DS appeared to be quite linear. However, the use of a mechanical stirrer instead of a magnetic stirrer resulted in a slightly higher DS. For instance, reaction with 120 mol% of acetyl sulfate resulted in 52% and 58% by using magnetic and mechanical stirring respectively. However, the differences were not significantly large considering experimental uncertainty.

Upon sulfonation, thermal properties of BCP membranes were changed. As shown in Fig. 3(a), DSC analyses of prestine SBS, sSBS-35% and sSBS-56% evidently showed that T_g of PS block increased from 78 °C to 99 °C and 108 °C with increased DSs while that of PB block did not changed much The observation implies that sulfonation occurred preferentially on PS block. It is reported that a significantly low T_g (~78 °C) of PS block in prestine SBS than that of homo-PS is due to a kinetic entrapment effect of minor PS block by rubbery center block [34,35]. As shown in Fig. 3(b), TGA measurements on the same samples revealed that both sSBS-35% and sSBS-56% exhibit low initial degradation temperature (~150 °C) while sharp weight loss occur at ~450 °C for both sSBS's which is significantly higher than that of prestine SBS. It was previously reported that unlike sulfonated PS, sSBS exhibits higher degradation temperature with increased DS due to an alternative degradation pathway of the BCP [35].

In the previous studies the BCP ionomers usually showed a percolation behavior in the plot of proton conductivity vs. DS due to the formation of proton conducting channels by fusion of ion clusters [18,19]. Fig. 4 is the overlaid plot of proton conductivities and water uptakes of sSBS membranes with varying DS. Proton conductivity of sSBS showed a dramatic increase at 40–50% of DS, and the maximum proton conductivity of 0.045 S/cm was obtained from sSBS-58% PEM. The water uptake data from four selected membranes were plotted together, which showed similar behavior of proton conductivity with DSs. In Fig. 4, a percolation

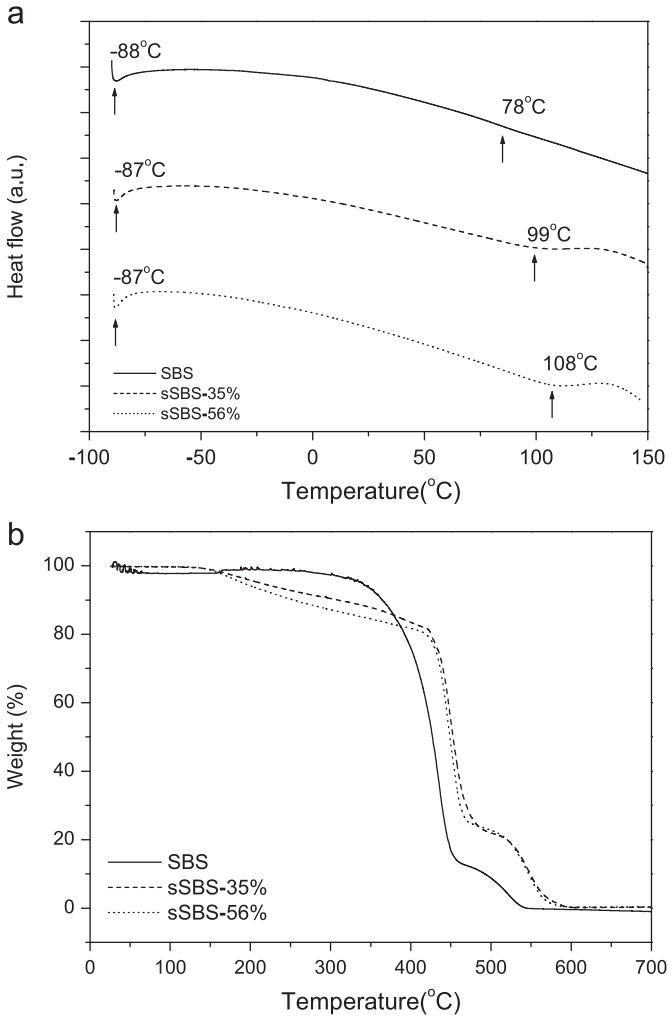

Fig. 3. Thermal properties of SBS, sSBS-35%, and sSBS-56% membranes. (a) Differential scanning calorimetry (DSC) thermogram, (b) Thermal gravimetric analysis (TGA) data. The arrows in DSC thermograms indicate T_g's of PB and PS blocks in each sample.

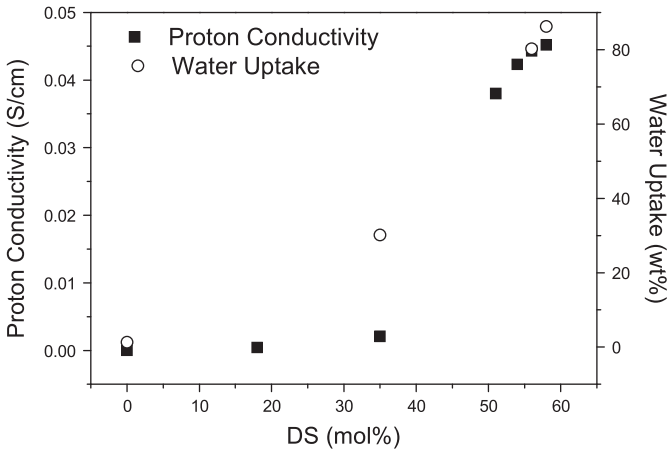

Fig. 4. Ion conductivity and water uptake as a function of DS of sSBS PEMs. Every measurement was carried out at room temperature.

threshold of sSBS ionomer system was determined to be around 35% of DS.

To elucidate structural information of sSBS block copolymer ionomers, SAXS study was carried out on the selected samples. The 10 μm-thick membranes were prepared by slow drying of the

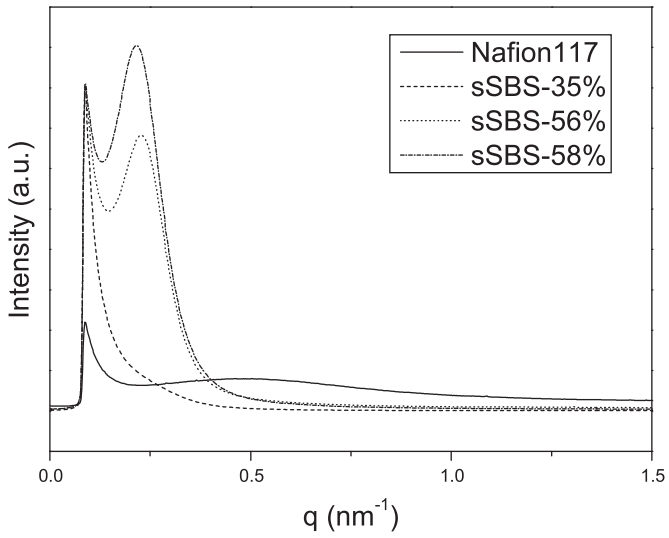

Fig. 5. Small-angle X-ray scattering data of the PEMs with various DS used in this study.

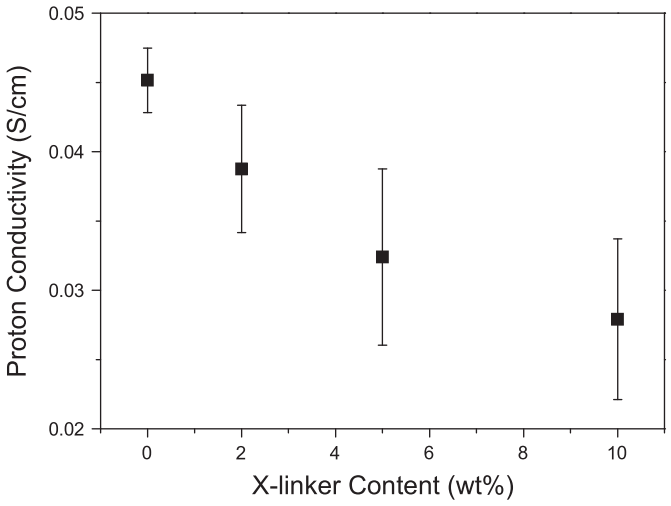

Fig. 6. Proton conductivities of sSBS-58% PEMs with various crosslinker content.

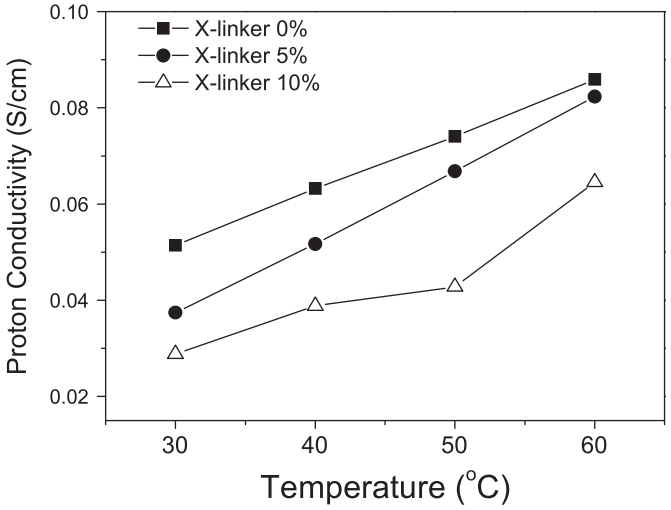

Fig. 7. Proton conductivities of the crosslinked sSBS-58% PEM at different temperatures.

mixed solvent of toluene/1-butanol. SAXS intensities vs. scattering vector (q) measured from three ionomer membranes with different DSs were plotted in Fig. 5, in which sSBS-56% and sSBS-58% showed strong scattering peaks at the q ranges of 0.24 nm^{-1} and 0.23 nm^{-1} while sSBS-35% exhibited no significant peak within the scanned q ranges. Development of SAXS peaks with increased DS can be explained by effective formation of ion channels beyond the percolation threshold. Presumably, sSBS-35% is still low in DS, and there are not enough ion clusters or channels to be recognized in a SAXS plot. It is noteworthy that the scattering peaks of sSBS-56% and 58% were found at lower angles than that of Nafion 117 membrane. The pristine SBS used in this study contains 29% of PS block, and the microphase separation of the BCP sample should exhibit cylindrical morphology [20]. By assuming that the developed ion channels maintain cylindrical microstructures, one can apply $d=(2\pi/q)\cdot(4/3)^{1/2}$ to the calculation of the intercylinder spacing [23]. The calculation reveals that q values of 0.23 nm^{-1} and 0.24 nm^{-1}, respectively correspond to 31.5 nm and 30.2 nm in intercylinder spacings.

In SAXS measurements, we also observed the decrease in q with hydration of an sSBS PEM (see Fig. S4), which can be attributed to an increased intercylinder spacing by swelling of the hydrophilic domains. The crosslinking of sSBS also resulted in the increased intercylinder spacing possibly due to the sequestration of DVB within PS domains. (Supporting data S3, 4) It is well known that the blending of low molecular weight species which is miscible with one or both blocks in a block copolymer results in the increase in inter-domain spacings [36]. The increased domain spacing by crosslinker was observed in both dry and wet membranes.

Fig. 6 shows that the proton conductivity of sSBS-58% decreases as the crosslinker content increases. Two main reasons can be addressed for such behaviors. First, a nonconducting DVB should behave as an impurity in a conducting medium. Second, the crosslinking keeps the PEMs from effective hydration and subsequent swelling, which actually helps the formation of proton conducting channels. In developing crosslinked PEM, one should consider trade-off characteristics between proton conductivity and chemical stability [18]. Crosslinking usually improves the chemical and mechanical stability (and fuel crossover) of the membrane, while sacrificing the proton conductivity.

As shown in Fig. 7, temperature-dependent proton conductivities of the crosslinked sSBS-58% membarnes were investigated. The non-crosslinked membrane showed higher conductivities over entire temperature range (30–60 °C), showing maximum proton conductivity of ~0.09 S/cm at 60 °C. The crosslinked PEM showed lower conductivity at 30 °C, but that of the PEM with 5% crosslinker remarkably increased and showed almost the same conductivity with the non-crosslinked membrane at 60 °C. van't Hoff analysis on these data revealed that the activation energy for proton conduction is slightly higher in the crosslinked membrane.

Mechanical strengths of the membranes were tested by plotting the tensile stress as a function of strain in uniaxial elongation measurement of sSBS-58%. As shown in Fig. 8, non-crosslinked sSBS-58% exhibited the lowest tensile stress, which gradually increased with crosslinker content. Nafion115 showed a lower tensile stress than that of sSBS-58% with 10% DVB, though a higher elongation. The results confirm that the inclusion of crosslinker improves the physical strength of the sSBS PEM. In Table 1, various properties of the crosslinked sSBS-58% membranes as well as tensile stresses at the break point are summarized. Among the listed properties in Table 1, membrane selectivity, the ratio of proton conductivity and methanol permeability of each PEM normalized to that of a Nafion membrane (Nafion 115 in this study) is very important as a PEM for DMFC. In Table 1, sSBS-58% PEMs apparently showed the membrane selectivity larger than unity regardless of

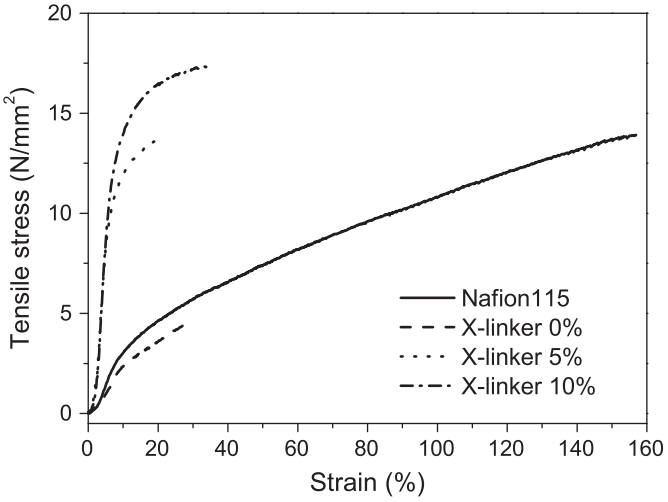

Fig. 8. Strain–stress curves of the crosslinked sSBS-58% PEM and Nafion-115. All the membranes were fully hydrated at room temperature before measurements.

crosslinking. As mentioned earlier, proton conductivity and methanol permeability have a trade-off relationship each other, and that is why we could not find a meaningful tendency in the membrane selectivity of sSBS PEMs with crosslinker content. Upon crosslinking, however, the mechanical properties were evidently improved. Table 1 shows that both water uptake and water swelling were diminished with respect to the crosslinker content, and contrarily, oxidative life-time of the PEMs in Fenton's reagent was obviously increased with crosslinker amounts showing an improvement of chemical resistance.

In order to test the sSBS PEMs developed in this study in an actual DMFC, MEAs were fabricated using crosslinked and non-crosslinked sSBS-58% [37]. For comparison, an MEA with Nafion 115 was also fabricated. After activating each single cell with 1 M methanol for 4 h, active mode DMFC performance curves were obtained in the temperature range between 30 and 60 °C. As shown in Fig. 9, non-crosslinked sSBS-58% PEM resulted in the maximum power density of 80 mW/cm^2 at 60 °C which is 15% higher than that of Nafion115. However, the power density of a single cell using a crosslinked sSBS-58% PEM appeared to be only 24 mW/cm^2 probably due to a lowered proton conductivity by addition of crosslinker. Considering that the fabrication procedure of the sSBS-containing MEA is actually the optimized one for Nafion-based MEA, the observed power performance of a non-crosslinked sSBS-58% ought to be noteworthy.

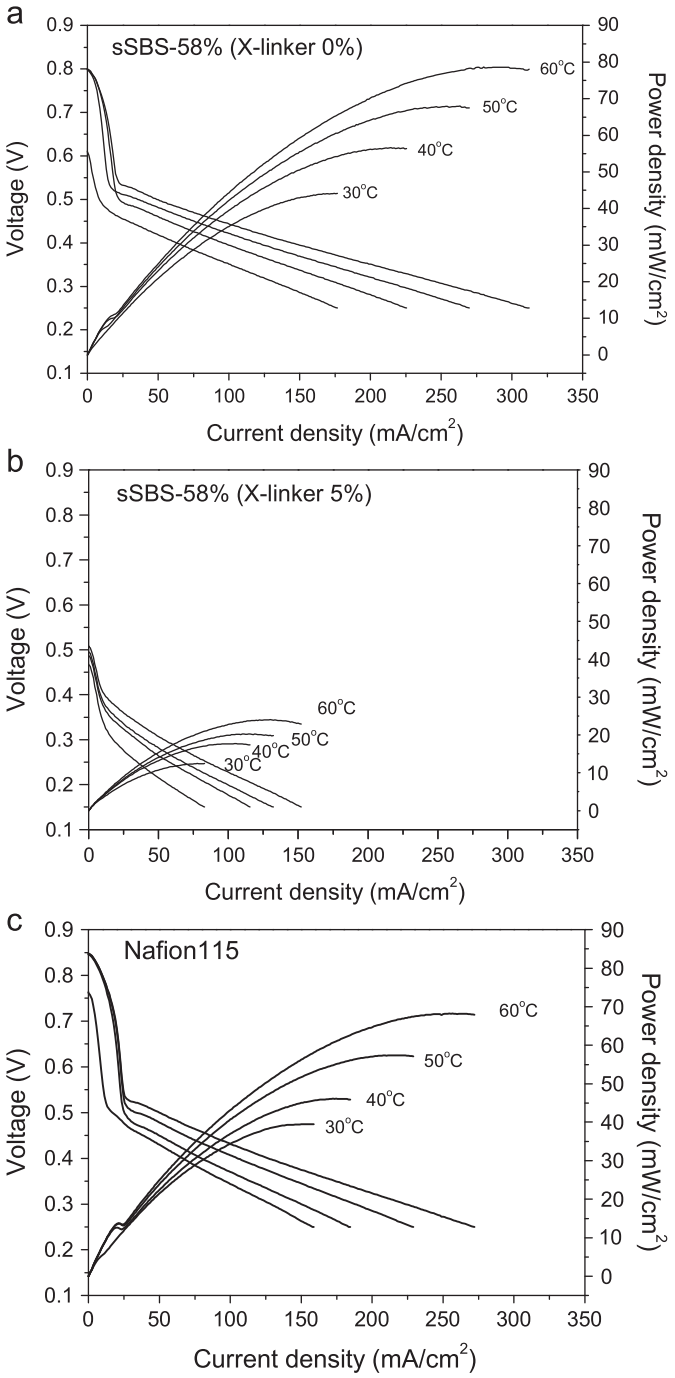

Fig. 9. Active mode DMFC performance curves of the MEAs using different PEMs.

4. Conclusions

Direct sulfonation of a commercial SBS block copolymer was investigated using acetyl sulfate for the preparation of an actual PEM for DMFC, and photo-crosslinking of the sSBS PEM with DVB was also carried out in order to improve mechanical stability of the block copolymer PEMs. The use of a mixed solvent of toluene/butanol resulted in a uniform solution of sSBS without significant gelation, and tough membranes were obtained by slow evaporation of the solvents. SAXS measurements revealed a successful formation of ionic channels of a highly sulfonated sSBS membrane, and an increased inter-domain spacing by mixing DVB crosslinker. By increasing the concentration of acetyl sulfate, sSBS with 58% DS was synthesized exhibiting a reasonably high proton conductivity (50% of Nafion 115) and a substantially improved methanol permeability. The crosslinking of sSBS PEMs showed improved chemical/mechanical stabilities of the cast membranes as confirmed by various tests, although the proton conductivity was a bit deteriorated due to an existence of non-ionic crosslinker within the membrane. MEA fabrication and active mode DMFC performance tests were carried out using crosslinked and non-crosslinked sSBS-58% PEMs, and the maximum power density of ~80 mW/cm^2 was obtained with an MEA containing non-crosslinked sSBS-58% which was a 15% better performance than Nafion 115 containing MEA.

Acknowledgment

The authors thank Dr. Seongyop Lim and Dr. Doo-Hwan Jung for helpful discussions. This work was supported by KOSEF through the Center for Electro-Photo Behaviors in Advanced

Molecular Systems (Grant number: 2012-0000532), and partially supported by the Basic Science Research Program through the National Research Foundation of Korea (NRF) funded by the Korea Government (MEST) (NRF-2009-C1AAA001-0093049 and R11-2005-048-00000-0).

Appendix A. Supporting information

Supplementary data associated with this article can be found in the online version at http://dx.doi.org/10.1016/j.memsci.2012.09.008.

References

[1] T. Schultz, S. Zhou, K. Sundmacher, Chem. Eng. Tech. 24 (2001) 1223.
[2] Y.A. Elabd, E. Napadensky, J.M. Sloan, D.M. Crawford, C.W. Walker, J. Membr. Sci. 217 (2003) 227.
[3] M. Rikukawa, K. Sanui, Prog. Polym. Sci. 25 (2000) 1463.
[4] A. Heinzel, V.M. Barragan, J. Power Sources 84 (1999) 70.
[5] C. Yang, S. Srinivasan, A.S. Arico, P. Creti, V. Baglio, V. Antonucci, Electrochem. Solid State Lett. 4 (2001) A31.
[6] S. Siracusano, V. Baglio, M.A. Navarra, S. Panero, V. Antonucci, A.S. Arico, Int. J. Electrochem. Sci. 7 (2012) 1532.
[7] N. Carretta, V. Tricoli, F. Picchioni, J. Membr. Sci. 166 (2000) 189.
[8] S.L. Zhong, X.J. Cui, H.L. Cai, T.Z. Fu, C. Zhao, H. Na, J. Power Sources 164 (2007) 65.
[9] S.M.J. Zaidi, S.D. Mikhailenko, G.P. Robertson, M.D. Guiver, S. Kaliaguine J. Membr. Sci. 173 (2000) 17.
[10] N. Asano, M. Aoki, S. Suzuki, K. Miyatake, H. Uchida, M. Watanabe, J. Am. Chem. Soc. 128 (2006) 1762.
[11] K. Ramya, B. Vishnupriya, K.S. Dhathathreyan, J. New Mater. Electrochem. Syst. 4 (2001) 115.
[12] F. Lufrano, G. Squadrito, A. Patti, E. Passalacqua, J. Appl. Polym. Sci. 77 (2000) 1250.
[13] F. Wang, M. Hickner, Y.S. Kim, T.A. Zawodzinski, J.E. McGrath, J. Membr. Sci. 197 (2002) 231.
[14] W.L. Harrison, F. Wang, J.B. Mecham, V.A. Bhanu, M. Hill, Y.S. Kim, J.E. McGrath, J. Polym. Sci. Part a 41 (2003) 2264.
[15] S.C. Gil, J.C. Kim, D. Ahn, J. Jang, H. Kim, J.C. Jung, S. Lim, D. Jung, W. Lee J. Membr. Sci. 417-418 (2012) 2.
[16] Y.A. Elabd, C.W. Walker, F.L. Beyer, J. Membr. Sci. 231 (2004) 181.
[17] J. Kim, B. Kim, B. Jung, J. Membr. Sci. 207 (2002) 129.
[18] W. Lee, S.C. Gil, H. Lee, H. Kim, Macromol. Res. 17 (2009) 451.
[19] W. Lee, H. Kim, H. Lee, J. Membr. Sci. 320 (2008) 78.
[20] J. Won, S.W. Choi, Y.S. Kang, H.Y. Ha, I.H. Oh, H.S. Kim, K.T. Kim, W.H. Jo J. Membr. Sci. 214 (2003) 245.
[21] S.Y. Kim, S. Kim, M.J. Park, Nat. Commun. 88 (2010) 1.
[22] S.Y. Kim, E. Yoon, T. Joo, M.J. Park, Macromolecules 44 (2011) 5289.
[23] J. Won, H.H. Park, Y.J. Kim, S.W. Choi, H.Y. Ha, I.H. Oh, H.S. Kim, Y.S. Kang, K.J. Ihn, Macromolecules 36 (2003) 3228.
[24] T. Brewer, AMAP 12th Annual Meeting, DeWitt & Company, 2011.
[25] A. Morkrini, J.L. Acosta, J. Appl. Polym. Sci. 83 (2002) 367.
[26] A. Mokrini, J.L. Acosta, Polymer 42 (2001) 9.
[27] B. Smitha, S. Sridhar, A.A. Khan, J. Membr. Sci. 225 (2003) 63.
[28] C.H. Rhee, H.K. Kim, H. Chang, J.S. Lee, Chem. Mater. 17 (2005) 1691.
[29] B.S. Pivovar, Y.X. Wang, E.L. Cussler, J. Membr. Sci. 154 (1999) 155.
[30] V. Tricoli, N. Carretta, M. Bartolozzi, J. Electrochem. Soc. 147 (2000) 1286.
[31] S.H. Kwak, T.H. Yang, C.S. Kim, K.H. Yoon, Solid State Ionics 160 (2003) 309.
[32] T. Kim, J. Kim, Y. Kim, T. Lee, W. Kim, K.S. Suh, Curr. Appl. Phys. 9 (2009) 120.
[33] H. Xie, D. Liu, D. Xie, J. Appl. Polym. Sci. 96 (2005) 1398.
[34] J.E. Kennedy, J.G. Lyons, L.M. Geever, C.L. Higginbotham, Mater. Sci. Eng. C 29 (2009) 1655.
[35] F. Picchioni, I. Giorgi, E. Passaglia, G. Ruggeri, M. Aglietto, Polym. Int. (2001) 714.
[36] A. Urbas, R. Sharp, Y. Fink, E.L. Thomas, M. Xenidou, L.J. Fetters, Adv. Mater. 12 (2000) 812.
[37] W. Lee, H. Kim, T.K. Kim, H. Chang, J. Membr. Sci. 292 (2007) 29.